

Two-Photon Circular–Linear Dichroism of Perylene in Solution: A Theoretical–Experimental Study

Marcelo G. Vivas,[†] Carlos Diaz,[‡] Lorenzo Echevarria,^{‡,§} Cleber R. Mendonca,[†] Florencio E. Hernández,^{*,‡,⊥} and Leonardo De Boni^{*,†}

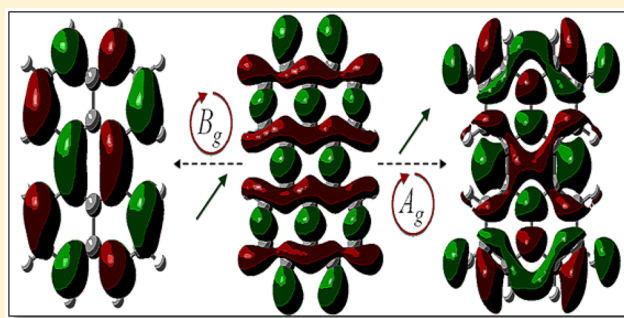
[†]Instituto de Física de São Carlos, Universidade de São Paulo, Caixa Postal 369, 13560-970 São Carlos, SP, Brazil

[‡]Department of Chemistry, University of Central Florida, P.O. Box 162366, Orlando, Florida 32816-2366, United States

[§]Departamento de Química, Universidad Simón Bolívar, Caracas 1020A, Venezuela

[⊥]CREOL/The College of Optics and Photonics, University of Central Florida, P.O. Box 162366, Orlando, Florida 32816-2366, United States

ABSTRACT: Herein, we report on the theoretical–experimental analysis of the two-photon absorption (TPA) and two-photon circular–linear dichroism (TPCLD) spectra of a highly conjugated, rigid, and centrosymmetric molecule in solution, that is, perylene/CH₂Cl₂. We show how a three-energy-level diagram, under the sum-over-essential states approach, assists in the determination of the magnitude of transition electric dipole moments and the angle between them for the main TPA transitions. We demonstrate the potential of TPCLD to reveal the symmetry of excited states and the angles between their transition electric dipole moments and that of the ground state. By means of TPCLD, we explain how the overwhelming contribution of certain TPA transitions can mask important spectral features in regions where the transition electric dipole moments are perpendicular. TPCLD is expected to enhance the understanding of the photophysical properties of materials that are not accessible using conventional linear and two-photon spectroscopy. TPA and TPCLD measurements were performed employing the open-aperture Z-scan technique using an amplified femtosecond system. Time-dependent density functional theory (TD-DFT) calculations were carried out using response theory at the B3LYP level with the aug-cc-pVDZ basis set. Solvent effects were included through the polarizable continuum model (PCM).



I. INTRODUCTION

During the past two decades, two-photon absorption (TPA)¹ has presented a significant growth in the scientific community because of two main reasons: (1) the many experimental and theoretical studies on this nonlinear optical effect^{2–5} that have led to the establishment of the basis for molecular engineering of two-photon absorbers, and (2) the numerous technological applications of TPA that have been found in the fields of photonics,^{6,7} biology,^{8,9} optical switches,^{10,11} and medicine¹² among others. These applications have been boosted by (a) the TPA quadratic dependence with the incident irradiance which confers more spatial resolution and penetration depth, and (b) the reduction of losses because of scattering and linear absorption when inducing an electronic excitation using two photons of longer wavelengths than those required for one-photon absorption (OPA). The different parity selection rules that govern TPA and OPA^{13,14} make these two approaches to be complementary spectroscopic techniques primarily in centrosymmetric molecules where these selection rules are strict. Since the transition probability of two-photon absorbers depends on the molecular structure and the molecular environment, TPA has become a powerful spectroscopic

technique to study the electronic structure of molecules with different structures. However, TPA has not yet been fully explored as a spectroscopic tool. In 1971, McClain showed,¹⁵ theoretically, the potential of polarization-dependent two-photon spectroscopy for the identification of the nature of the excited states of randomly oriented molecules. These types of studies remained in obscurity for decades until fresh theoretical¹⁶ and experimental^{17,18} work primarily done on chemical and biological chiral systems using two-photon circular dichroism (TPCD)^{19,20} and two-photon circular–linear dichroism (TPCLD)^{17,21} resuscitated it. TPCD is defined as $\Delta\delta^{\text{TPCD}}(\lambda) = \delta_{\text{L}}^{\text{TPA}}(\lambda) - \delta_{\text{R}}^{\text{TPA}}(\lambda)$, where $\delta_{\text{L}}^{\text{TPA}}(\lambda)$ and $\delta_{\text{R}}^{\text{TPA}}(\lambda)$ are the TPA cross sections, $\delta^{\text{TPA}}(\lambda)$, for left and right circularly polarized light. TPCLD is defined as $\Delta\delta^{\text{TPCLD}}(\lambda) = [\Omega_{\text{CLD}}^{\text{TPA}}(\lambda) - 1]/[\Omega_{\text{CLD}}^{\text{TPA}}(\lambda) + 1]$, where $\Omega_{\text{CLD}}^{\text{TPA}} = \delta_{\text{CP}}^{\text{TPA}}(\lambda)/\delta_{\text{LP}}^{\text{TPA}}(\lambda)$ is the ratio between the TPA cross section obtained using circularly ($\delta_{\text{CP}}^{\text{TPA}}(\lambda)$) and linearly ($\delta_{\text{LP}}^{\text{TPA}}(\lambda)$) polarized light. While TPCD is a specific property for optically active samples because it

Received: November 8, 2012

Revised: February 1, 2013

Published: February 5, 2013

depends directly on the transition magnetic dipole moment and the transition electric quadrupole moment, TPCLD is not purely chiral because it is governed by the transition electric dipole moment. Consequently, TPCLD could be considered as a more general approach than TPCD opening access to the determination of the angle between transition electric dipole moments²² and the symmetry of excited states²³ of achiral samples (since right and left circular polarization are identical within the electric dipole approximation, one can use either one in nonoptically active samples). In addition, it has recently been demonstrated that TPA polarization microscopy provides higher responsiveness than conventional TPA microscopy.²⁴ Therefore, further systematic studies on organic molecules using polarization-dependent TPA spectroscopy are in great demand to gain a deeper understanding of the photophysical properties of materials that are not accessible using conventional OPA and TPA spectroscopy.

To expand the knowledge in this field, we recently engaged in the study of a highly conjugated, rigid, and centrosymmetric molecule in solution using TPCLD. Herein, we report on the theoretical–experimental study of TPA and TPCLD spectra of perylene in CH₂Cl₂ solution employing the open-aperture Z-scan technique in the femtosecond regime and performing quantum chemical calculations using time-dependent density functional theory (TD-DFT).

II. EXPERIMENTAL PROCEDURES

Perylene and CH₂Cl₂ were purchased from Fischer Scientific and were used without any further purification. The OPA spectrum was measured in an 8.3×10^{-5} M solution with a Shimadzu UV-1800 spectrophotometer (2 mm thick quartz cuvette, solvent and cell effects were subtracted). The nonlinear optical measurements were performed using the open-aperture Z-scan technique in a 1.7 mM solution. The TPA measurements for the TPCLD determination were performed with an optical parametric amplifier pumped by the fundamental (775 nm) of a Ti:sapphire chirped pulse amplified system operating at 1 kHz repetition rate and a pulse width of 150 fs (fwhm). The covered spectral range was 400–800 nm. Z-scan measurements were carried out pumping at intensities ranging from 100 to 300 GW/cm² (50–180 nJ/pulse) and at a Gaussian beam with focal plane waist between 14 to 17 μ m (fwhm). The excitation polarization state was controlled using a broad band zero-order quarter-wave plate.

Since TPCLD is a nonlinear optical effect that is governed by the electric dipole moment, the difference between the TPA cross sections using circularly and linearly polarized light is significantly large in most molecules. Therefore, the TPCLD signal can be easily determined by employing the well-known open-aperture Z-scan. In the present work, the TPA measurements using circularly and linearly polarized light were performed independently in separated runs. Afterward, the recovered TPA cross sections were combined according to the equation that defines TPCLD ($\Delta\delta^{\text{TPCLD}}(\lambda) = [\Omega_{\text{CLD}}^{\text{TPA}}(\lambda) - 1]/[\Omega_{\text{CLD}}^{\text{TPA}}(\lambda) + 1]$). Figure 1 shows typical open-aperture Z scan curves measured using linearly polarized (LP) (diamonds) and circularly polarized (CP) (squares) light at three different wavelengths.²⁵ The difference in TPA using CP and LP depends on the excitation wavelength.

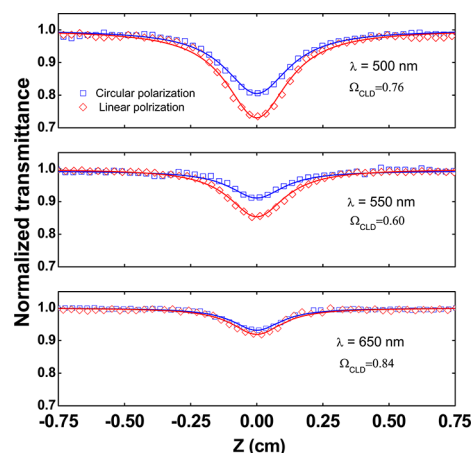


Figure 1. Open-aperture Z-scan curves in a perylene solution using linearly (red diamonds) and circularly (blue squares) polarized light. The solid lines represent the theoretical fitting employing the theory described in ref 25.

III. COMPUTATIONAL AND THEORETICAL METHODS

III.A. Time-Dependent Density Functional Theory (TD-DFT) Calculations. The molecular structure of perylene was optimized using density functional theory (DFT) in Gaussian 09²⁶ employing the Becke's three-parameter exchange Lee, Yang, and Parr correlation (B3LYP) hybrid functional^{27–29} and the 6-31G(d) basis set.³⁰ The optimized structure was utilized to calculate the degenerate (photons of equal frequency) TPA response for the lowest 16 electronic excited states with LP and CP light. These calculations were performed in Dalton 2011³¹ using time-dependent DFT (TD-DFT) with the B3LYP hybrid functional and basis set aug-cc-pVDZ.³² The polarizable continuum model (PCM) was used in all calculations to account for solvent effects.³³

The orientational averaged TPA probability ($\bar{\delta}_{0f}^{\text{TPA}}(\omega_{0f})$) for the degenerate case is given by¹⁵

$$\bar{\delta}_{0f}^{\text{TPA}}(\omega_{0f}) = \sum_{\alpha\beta} (F \times S_{\alpha\alpha}^{0f} S_{\beta\beta}^{*,0f} + G \times S_{\alpha\beta}^{0f} S_{\alpha\beta}^{*,0f} + H \times S_{\alpha\beta}^{0f} S_{\beta\alpha}^{*,0f}) \quad (1)$$

where the two-photon excitation takes place from the ground state $|0\rangle$ to a final excited state $|f\rangle$. The $\alpha\beta$ element of the two-photon tensor $S_{\alpha\beta}^{0f}$ depends on the circular frequency $(\omega_{0f})/2$, and F , G , and H are scalars used to define the polarization of light ($F = G = H = 2$ for LP and $F = -2$, $G = 3$, and $H = 3$ for CP).

Because of the symmetry of the TPA tensor, eq 1 simplifies to

$$\bar{\delta}_{0f}^{\text{TPA}}(\omega_{0f}) = FA(\omega_{0f}) + (G + H)B(\omega_{0f}) \quad (2)$$

where $A(\omega_{0f}) = (1/30) \sum_{\alpha\beta} S_{\alpha\alpha}^{0f} S_{\beta\beta}^{*,0f}$ and $B(\omega_{0f}) = (1/30) \sum_{\alpha\beta} S_{\alpha\beta}^{0f} S_{\alpha\beta}^{*,0f}$ and $\bar{\delta}_{0f}^{\text{TPA}}(\omega_{0f})$ is given in atomic units.

The TPA cross section spectra for both LP and CP were obtained using eq 3^{15,34,35}

$$\delta_{0f}^{\text{TPA}}(\omega) = \frac{4\pi^3 \alpha a_0^5}{c} \sum_f (\hbar\omega_f)^2 \bar{\delta}_{0f}^{\text{TPA}}(\omega_{0f}) g(2\omega, \omega_{0f}, \Gamma) \quad (3)$$

where α is the fine structure constant, a_0 is the Bohr's radius, c is the speed of light, and $E = \hbar\omega$ is the photon energy (half of

the transition energy). $g(2\omega, \omega_{0f}, \Gamma)$ represents the line-shape function of the final excited state. Here, we have used a Lorentzian function given by

$$g(2\omega, \omega_{0f}, \Gamma) = \frac{1}{\pi} \frac{\Gamma_{g_f}}{(\omega_{g_f} - 2\omega)^2 + (\Gamma_{g_f})^2} \quad (4)$$

where Γ is the damping constant described as the half width at half-maximum (HWHM) of the final state line width. All calculated transitions were broadened using $\Gamma = 0.2$ eV ($\sim 5.0 \times 10^{13}$ s $^{-1}$ or $\sim 7.5 \times 10^{-3}$ atomic units). This specific value was estimated from the experimental TPA spectra. To obtain the TPA cross section in Göppert–Mayer units, in eq 3 one has to use $a_0 = 5.291772108 \times 10^{-9}$ cm and $c = 2.99792458 \times 10^{10}$ cm/s and the values of $E = \hbar\omega$, Γ_f and $\delta_{0f}^{\text{TPA}}(\omega_{0f})$ in atomic units.

By merging the TPCLD definition with eqs 2 and 3, one can obtain the following simple expression for the theoretical TPCLD spectra written in terms of $A(\omega_{0f})$ and $B(\omega_{0f})$ ^{16–20}

$$\Delta\delta^{\text{TPCLD}}(\omega) = \frac{\sum_f g(2\omega, \omega_{0f}, \Gamma) \cdot (-2A(\omega_{0f}) + B(\omega_{0f}))}{\sum_f g(2\omega, \omega_{0f}, \Gamma) \cdot (5B(\omega_{0f}))} \quad (5)$$

III.B. Sum-Over-Essential States Approach (SOS). In most cases, a quantitative interpretation of the experimental TPA cross section spectrum can be accomplished taking into account only a few energy levels (essential states, i.e., states with higher TPA probabilities). Because it is very difficult to obtain with precision information about all electronic states, our approach consists of considering only the states with higher TPA probability.^{36,37} On the basis of this statement, here we used a three-energy-level diagram to fit the TPA experimental spectra obtained using LP and CP. In this model, the ground state, $|0\rangle$, represents the first level while an OPA allowed real intermediate state, $|1\rangle^{\text{OPA}}$, and the TPA allowed final state, $|f_i\rangle^{\text{TPA}}$, represent the third level (see diagram in the inset of Figure 4). Using this energy diagram and considering an average over all possible molecular orientations in an isotropic medium, the TPA cross section (in GM units) for centrosymmetric molecules can be written as^{22,38}

$$\delta_{g \rightarrow f_i}^{(\text{TPA})}(2\omega) = (1 \times 10^{-22}) 2 \frac{(2\pi)^5}{(nhc)^2} L^4 P(\theta) R(\omega) |\vec{\mu}_{01}|^2 |\vec{\mu}_{1f_i}|^2 g_{g_f}(2\omega, \omega_{g_f}, \Gamma) \quad (6)$$

where h (erg·s) is the Planck's constant, c (cm·s $^{-1}$) is the speed of light, and $L = 3n^2/(2n^2 + 1)$ is the Onsager local field factor introduced to take into account the medium effect with $n = 1.42$ for CH₂Cl₂. $P(\theta) = \{[2 \cos^2(\theta_{\vec{\mu}_{01}\vec{\mu}_{1f_i}}) + 1]/15\}$ for linear polarization, and $P(\theta) = \{[\cos^2(\theta_{\vec{\mu}_{01}\vec{\mu}_{1f_i}}) + 3]/30\}$ for circular polarization. $R(\omega) = \omega^2/[(\omega_{01} - \omega)^2 + \Gamma_{01}^2]$ is the resonance enhancement factor (dimensionless), and $\theta_{\vec{\mu}_{01}\vec{\mu}_{1f_i}}$ is the angle between the transition electric dipole moments $\vec{\mu}_{01}$ and $\vec{\mu}_{1f_i}$ (in Debye; 1 D = 1×10^{-18} erg $^{1/2}$ ·cm $^{3/2}$). Within the three-energy-level approach, $\theta_{\vec{\mu}_{01}\vec{\mu}_{1f_i}}$ can be obtained using eq 7.

$$\theta_{\vec{\mu}_{01}\vec{\mu}_{1f_i}} = \arccos \left(\frac{3 - 2\Omega_{\text{CLD}_i}^{\text{TPA}}}{4\Omega_{\text{CLD}_i}^{\text{TPA}} - 1} \right)^{1/2} \quad (7)$$

$\Omega_{\text{CLD}_i}^{\text{TPA}} = \sigma_{\text{TPA}_i}^{\text{CP}}/\sigma_{\text{TPA}_i}^{\text{LP}}$ is the ratio between the TPA cross section obtained using circular and linear polarization light. The transition electric dipole moment, $|\vec{\mu}_{01}|$ (in Debye), is assessed directly from the molar absorptivity spectrum using the following eq 8.

$$|\vec{\mu}_{01}|^2 = (1 \times 10^{36}) \frac{3 \times 10^3 \ln(10) hc}{(2\pi)^2 N_A} \frac{n}{L^2} \left(\frac{\pi \Gamma_{g_f}}{2} \right) \frac{\epsilon(\omega_{01})}{\omega_{01}} \quad (8)$$

Here, $\epsilon(\omega_{01})$ (M $^{-1}$ ·cm $^{-1}$) is the peak molar absorptivity at the transition frequency, ω_{01} (s $^{-1}$), and N_A (mol $^{-1}$) is the Avogadro's number. Finally, the transition electric dipole moment, $|\vec{\mu}_{1f_i}|$, can be estimated through the theoretical fitting of the experimental TPA spectra using eq 6.

Although the SOS approach is a simplified model, in conjunction with quantum chemical calculations, it has proven to be a powerful tool to determine molecular parameters of organic molecules giving a reasonable interpretation to the nonlinear absorption spectrum.^{13,34,35}

IV. RESULTS AND DISCUSSION

Figure 2 shows the OPA and the TPA spectra of perylene in CH₂Cl₂. The lowest energy band observed in the OPA

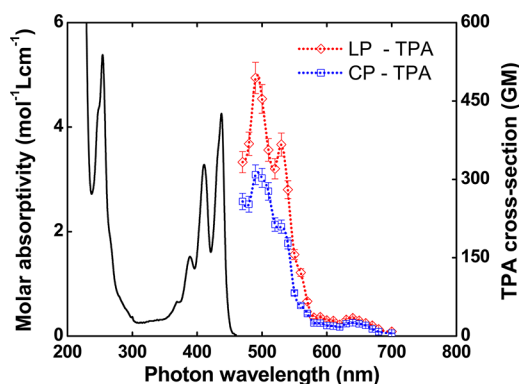


Figure 2. Experimental OPA (black solid line) and TPA spectra of perylene in CH₂Cl₂ for LP (red diamonds) and CP (blue squares). Dotted lines over the TPA data points are shown to guide the reader through the TPA spectra.

spectrum at approximately 438 nm (molar absorptivity 4×10^3 mol $^{-1}$ ·L·cm $^{-1}$) displays a well-resolved vibrational structure with a total of four peaks separated by approximately 170 meV. The cited features, spanning from 350 to 440 nm, are attributed to an effective internal vibrational mode in perylene.^{39,40} The TPA spectra exhibit two distinct bands: one weak located at ca. 640 nm and one strong between 470 and 580 nm containing a vibrational structure with a separation between the peaks of approximately 190 meV. This vibrational structure is equivalent to that observed in the OPA spectrum and has already been associated, in perylene derivatives, with transitions between nonlocalized conjugated states.⁴¹ It is important to emphasize that in centrosymmetric molecules, like perylene, there is no correspondence between the OPA and TPA spectra because parity selection rules are very strict (different parity for OPA and equal parity for TPA).¹⁴

The corresponding experimental TPA cross section values at the two main bands observed at 640 and 500 nm were (36 ± 5) GM and (500 ± 50) GM for LP light, respectively, and $(25 \pm$

5) GM and (315 ± 30) GM for CP light, correspondingly. As it can be seen in Figure 2, the TPA cross sections obtained for CP light, over the whole spectral range, are smaller than those for LP. Such differences can be correlated with the excited state molecular geometry adopted by perylene in solution.²³

To expand our understanding on the polarization-dependent two-photon spectroscopy, we calculated the theoretical TPA and the TPCLD spectra of perylene/ CH_2Cl_2 using TD-DFT and over the lowest TPA allowed 16 excited states. Figure 3

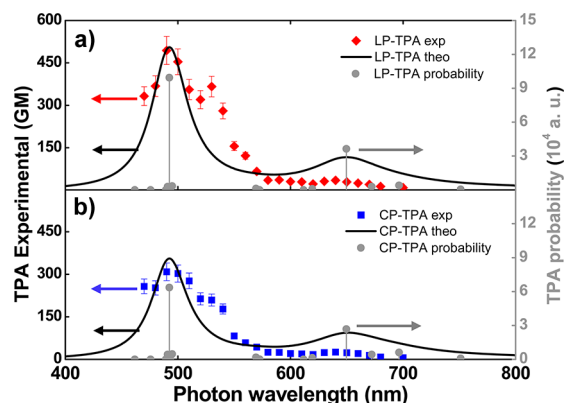


Figure 3. Experimental TPA spectra of perylene in CH_2Cl_2 for (a) LP and (b) CP with theoretical TPA electronic transitions and their Lorentzian convolution [line width 0.2 eV HWHM] (black solid line). The scattered black spheres show the TPA probability obtained from eq 2 for each specific transition. The theoretical spectra are shifted +50 nm.

displays the theoretical (solid lines) and experimental TPA spectra using LP (Figure 3a) and CP (Figure 3b) (to show better the agreement between theory and experiment, the theoretical curves were red-shifted 50 nm). In Figure 3, the scattered black spheres show the TPA probability obtained from eq 2 for each specific transition. Table 1 shows the TPA cross sections using LP and CP and their corresponding ratio,

$\Omega_{\text{CLD}}^{\text{TPA}}$. Among the calculated electronic states, S_4 (599 nm) and S_{11} (442 nm) present the highest TPA cross section values: S_4 (92 GM for LP and 68 GM for CP) and S_{11} (462 GM for LP and 296 GM for CP). Although transitions to these two excited states are in agreement with those revealed by the experiment, a spectral blue shift of ca. 50 nm and strong overestimation of the TPA cross section correspondent to the lowest energy band can be noticed (see Figure 3). On the one hand, the spectral shift can be justified by recognizing that theoretical calculations, using PCM to include solvent effects, are performed under the Lorentz–Lorenz approximation and do not consider specific solute–solvent interactions. On the other hand, the larger theoretical TPA cross section can be attributed to imprecisions in the determination of the line widths and transition energy.⁴²

The direct comparison between the experimental TPA spectra using LP and CP indicates that the TPA cross sections of the former are larger than those of the latter throughout the entire spectral range. This unanticipated result suggests that $\Omega_{\text{CLD}}^{\text{TPA}} < 1$ for all transitions. However, from Table 1, it is evident that $\Omega_{\text{CLD}}^{\text{TPA}} = 1.5$ for most transitions. According to theoretical results reported by Nascimento²³ on the polarization dependence of TPA rates for randomly oriented molecules, $0 \leq \Omega_{\text{CLD}}^{\text{TPA}} < 1$ for $0^\circ \leq \theta_{\vec{\mu}_{01}\vec{\mu}_{1fi}} < 54.7^\circ$, $1 \leq \Omega_{\text{CLD}}^{\text{TPA}} < 1.5$ for $54.7^\circ \leq \theta_{\vec{\mu}_{01}\vec{\mu}_{1fi}} < 90^\circ$, and $\Omega_{\text{CLD}}^{\text{TPA}} = 1.5$ for $\theta_{\vec{\mu}_{01}\vec{\mu}_{1fi}} = 90^\circ$ with $\theta_{\vec{\mu}_{01}\vec{\mu}_{1fi}}$ the angle between the transition electric dipole moments $\vec{\mu}_{01}$ and $\vec{\mu}_{1fi}$ (see eqs 4 and 5). Nascimento also showed that $\theta_{\vec{\mu}_{01}\vec{\mu}_{1fi}} = 90^\circ$ corresponds to transitions between states of different symmetry while $\theta_{\vec{\mu}_{01}\vec{\mu}_{1fi}} < 90^\circ$ corresponds to transitions between states of the same symmetry. Therefore, the main TPA bands observed in perylene should correspond to transitions between states with the same symmetry; moreover, since S_4 and S_{11} have A_g symmetry (see Table 1), the ground state must be of A_g symmetry as well. To corroborate this outcome, the TPA spectra of perylene/ CH_2Cl_2 , using LP and CP, were modeled using SOS and the energy diagram shown in the inset of Figure 4 (a normalized Lorentzian line shape

Table 1. Summary of Results for the TPA Theoretical Calculation^a

<i>n</i>	<i>symm.</i>	λ (nm)	$A(\omega_{0f})$ (a.u.)	$B(\omega_{0f})$ (a.u.)	$\delta_{0f,LP}^{\text{TPA}}(\omega_{0f})$ (GM)	$\delta_{0f,CP}^{\text{TPA}}(\omega_{0f})$ (GM)	$\Omega_{\text{CLD}}^{\text{TPA}}$
S_1	B_{1g}	700.565	0.00×10^0	1.47×10^{02}	1.09×10^{00}	1.63×10^{00}	1.50
S_2	B_{1g}	645.833	0.00×10^0	1.02×10^{03}	8.91×10^{00}	1.34×10^{01}	1.50
S_3	B_{1g}	621.554	0.00×10^0	7.17×10^{02}	6.75×10^{01}	1.01×10^{01}	1.50
S_4	A_g	599.034	5.55×10^{03}	6.31×10^{03}	9.21×10^{01}	6.78×10^{01}	0.74
S_5	B_{1g}	568.807	0.00×10^0	2.29×10^{02}	2.57×10^{00}	3.84×10^{00}	1.50
S_6	A_g	561.086	9.68×10^{-01}	3.47×10^{00}	4.56×10^{-02}	5.45×10^{-02}	1.19
S_7	B_{3g}	522.105	0.00×10^0	1.87×10^{01}	2.49×10^{-01}	3.73×10^{-01}	1.50
S_8	B_{2g}	518.828	0.00×10^0	3.09×10^{02}	4.15×10^{00}	6.24×10^{00}	1.50
S_9	A_g	444.444	1.01×10^{02}	8.27×10^{02}	1.61×10^{01}	2.19×10^{01}	1.36
S_{10}	B_{3g}	442.857	0.00×10^0	3.42×10^{-02}	6.35×10^{-04}	9.42×10^{-04}	1.50
S_{11}	A_g	442.068	1.71×10^{04}	1.63×10^{04}	4.62×10^{02}	2.96×10^{02}	0.64
S_{12}	B_{2g}	441.281	0.00×10^0	5.47×10^{02}	1.02×10^{01}	1.53×10^{01}	1.50
S_{13}	B_{2g}	440.497	0.00×10^0	7.20×10^{02}	1.35×10^{01}	2.02×10^{01}	1.50
S_{14}	B_{3g}	438.938	0.00×10^0	1.03×10^{00}	1.95×10^{-02}	2.93×10^{-01}	1.50
S_{15}	B_{3g}	425.386	0.00×10^0	1.87×10^{-01}	3.75×10^{-03}	5.62×10^{-03}	1.50
S_{16}	B_{2g}	411.277	0.00×10^0	4.12×10^{00}	8.86×10^{-02}	1.33×10^{-01}	1.50

^a *n* is the excited state number; *symm.* is the symmetry or irreducible representation; $A(\omega_{0f})$ (au) and $B(\omega_{0f})$ (au) are molecular parameters; $\delta_{0f,LP}^{\text{TPA}}(\omega_{0f})$ (GM) and $\delta_{0f,CP}^{\text{TPA}}(\omega_{0f})$ (GM) are the TPA cross sections for LP and CP, respectively; and $\Omega_{\text{CLD}}^{\text{TPA}} = \delta_{0f,CP}^{\text{TPA}}(\omega_{0f})/\delta_{0f,LP}^{\text{TPA}}(\omega_{0f})$ is the ratio between the TPA cross section obtained using CP and LP. The TPA cross sections ($\delta_{0f,LP}^{\text{TPA}}(\omega_{0f})$ (GM) and $\delta_{0f,CP}^{\text{TPA}}(\omega_{0f})$ (GM)) were computed adopting line width values estimated through the fit of the nonlinear spectra ($\Gamma = 0.2$ eV).

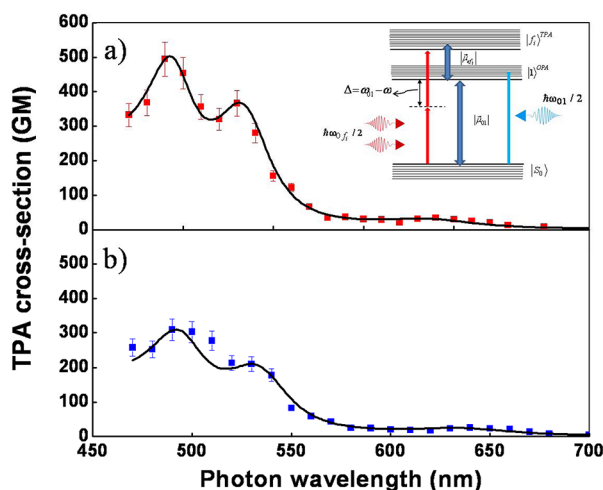


Figure 4. Experimental TPA spectra of perylene in CH_2Cl_2 for (a) LP and (b) CP with SOS fitting (black solid line). The inset in a shows the energy diagram used in the SOS approach to model the TPA spectra.

function with $\Gamma_{gf_i} = 0.2$ eV (HWHM) was employed). Figure 4 displays the experimental TPA spectra using LP and CP light and the corresponding curves generated with SOS. To estimate the angle between the transition electric dipole moments at the two main bands, we used eq 7. We found a $\theta_{\vec{\mu}_{01}\vec{\mu}_{1f1}} = 45^\circ \pm 15^\circ$ for the lowest energy transition (640 nm) and a $\theta_{\vec{\mu}_{01}\vec{\mu}_{1f2}} = 32^\circ \pm 10^\circ$ for the highest energy transition (500 nm). The magnitudes of the corresponding transition electric dipole moments were determined using the linear absorption spectrum along with eq 8 and fitting eq 6 in that order. This procedure yielded a $|\vec{\mu}_{01}| = 6.5$ D at the 430 nm OPA peak and $|\vec{\mu}_{1f1}| = 4.0$ D and $|\vec{\mu}_{1f2}| = 5.5$ D at the main TPA bands centered at 640 and 500 nm, respectively. The fact that the estimated $\theta_{\vec{\mu}_{01}\vec{\mu}_{1f1}}$ are between 0° and 54.7° reveals that the ground state and the corresponding excited states have the same symmetry. Furthermore, this result implies that $\Omega_{\text{CLD}}^{\text{TPA}} < 1$ for both transitions. However, according to the theoretical $\Omega_{\text{CLD}}^{\text{TPA}}$ reported in Table 1, one should expect many transitions for which $\sigma_{\text{TPA}_i}^{\text{CP}} > \sigma_{\text{TPA}_i}^{\text{LP}}$, that is, transitions between states with perpendicular transition electric dipole moments.

To explain the discrepancy found between the theoretical and the experimental $\Omega_{\text{CLD}}^{\text{TPA}}$, we measured the TPCLD spectrum of perylene in CH_2Cl_2 solution (see Figure 5). This novel and powerful spectroscopic technique can be used to gain information about the symmetry of the excited states and the relative orientation between transition electric dipole moments.

The first aspect to be highlighted in Figure 5 is the good spectral agreement between the theoretical and experimental TPCLD spectra. The theory clearly reproduces the broad peak between 580 and 720 nm (shoulder inclusive), the valley close to the center of the spectrum at 560 nm, and the smaller broad peak on the blue side of the spectrum between approximately 460 and 550 nm (shoulder inclusive). The nearly 2-fold difference in magnitude between the two spectra is attributed to the same factors described in Results and Discussion given above on the TPA spectra. The second, and perhaps the most important, aspect is the fact that both the theoretical and the experimental TPCLD spectra only show negative values ($\Delta\delta^{\text{TPCLD}} < 0$) within the investigated wavelength range.

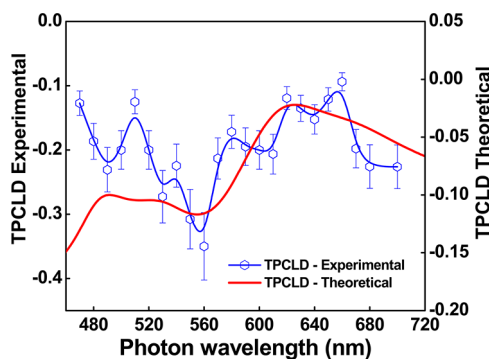


Figure 5. Experimental (diamonds) and theoretical (solid line) TPCLD spectra of perylene in CH_2Cl_2 . Theoretical and experimental TPCLD are displayed on different scales. The solid line along the diamonds is a guide to the reader. Theoretical TPCLD spectrum is shifted -35 nm.

These results seem to confirm the outcome regarding $\Omega_{\text{CLD}}^{\text{TPA}} < 1$ for all transitions discussed above. However, our theoretical calculations on the TPA allowed transitions in perylene, a molecule with symmetry point group D_{2h} ,⁴³ show that only 4 out of the 16 calculated excited states present a symmetry equal to that of the ground state (A_g); the other 12 have a different symmetry (B_{ig}). Because a negative TPCLD signal ($\Delta\delta^{\text{TPCLD}} < 0$, i.e., $\Omega_{\text{CLD}}^{\text{TPA}} < 1$) is only expected for transitions between states of the same symmetry,²³ one should anticipate a positive TPCLD in perylene within the spectral region corresponding to $A_g \rightarrow B_{ig}$ transitions (see Table 1). In fact, for transitions between states of different symmetry, $\Delta\delta^{\text{TPCLD}} = 0.2$, that is, $\Omega_{\text{CLD}}^{\text{TPA}} = 1.5$.²³ The predominance of negative TPCLD regions in the spectrum can be explained by the broadening of the TPA allowed states (bands) of perylene in solution because of all possible mechanisms of homogeneous and inhomogeneous broadening.⁴⁴ Consequently, transitions with a greater TPA cross section can have an overwhelming weight onto the shape and sign of the TPCLD spectrum, which also depends on the line width of the Lorentzian function. This is the case in perylene, where transitions to excited states S_4 and S_{11} are significantly stronger than the rest of the TPA allowed transitions (see Table 1). In addition, since these are $A_g \rightarrow A_g$ transitions, their negative TPCLD signal dictates the sign of the entire spectrum regardless of the existence of $A_g \rightarrow B_{ig}$ transitions.

V. SUMMARY

The experimental–theoretical TPA spectra of perylene, a well-known molecule with symmetry point group D_{2h} , have permitted the determination of the symmetry of the TPA allowed excited states and the angle between their transitions electric dipole moments. The estimation of $\theta_{\vec{\mu}_{01}\vec{\mu}_{1f1}}$ and $\vec{\mu}_{1f1}$ and $\vec{\mu}_{1f2}$ using a three-energy-level diagram and the SOS approach corroborated our results. The experimental–theoretical TPCLD signal helped to elucidate the apparent discrepancies in symmetry of the states involved in the allowed TPA transitions in perylene/ CH_2Cl_2 and the angle between their transition electric dipole moments. TPCLD has proven its potential as a nonlinear spectroscopic technique for the characterization of achiral molecules.

AUTHOR INFORMATION

Corresponding Author

*E-mail: deboni@ifsc.usp.br (L.D.B.) and florenzi@ucf.edu (F.E.H.).

Notes

The authors declare no competing financial interest.

ACKNOWLEDGMENTS

This work was partially supported by FAPESP (Fundação de Amparo à Pesquisa do estado de São Paulo), CNPq (Conselho Nacional de Desenvolvimento Científico e Tecnológico), Coordenação de Aperfeiçoamento de Pessoal de Nível Superior (CAPES), the Air Force Office of Scientific Research, and the National Science Foundation through Grant Number CHE-0832622. F.E. Hernandez would like to thank Dr. Sergio Tafur (STOKES ARCC) and Mr. Haining Wang (Chemistry Department) for their assistance in implementing Dalton 2011 at UCF.

REFERENCES

- Goeppert-Mayer, M. *Ann. Phys.* **1931**, *8*, 273–294.
- Albota, M.; Beljonne, D.; Bredas, J. L.; Ehrlich, J. E.; Fu, J. Y.; Heikal, A. A.; Hess, S. E.; Kogej, T.; Levin, M. D.; Marder, S. R.; et al. *Science* **1998**, *281*, 1653–1656.
- Hales, J. M.; Matichak, J.; Barlow, S.; Ohira, S.; Yesudas, K.; Bredas, J. L.; Perry, J. W.; Marder, S. R. *Science* **2010**, *327*, 1485–1488.
- Marder, S. R.; Gorman, C. B.; Meyers, F.; Perry, J. W.; Bourhill, G.; Bredas, J. L.; Pierce, B. M. *Science* **1994**, *265*, 632–635.
- Friedrich, D. M. *J. Chem. Educ.* **1982**, *59*, 472–481.
- Cumpston, B. H.; Ananthavel, S. P.; Barlow, S.; Dyer, D. L.; Ehrlich, J. E.; Erskine, L. L.; Heikal, A. A.; Kuebler, S. M.; Lee, I. Y. S.; McCord-Maughon, D.; et al. *Nature* **1999**, *398*, 51–54.
- Parthenopoulos, D. A.; Rentzepis, P. M. *Science* **1989**, *245*, 843–845.
- Denk, W.; Strickler, J. H.; Webb, W. W. *Science* **1990**, *248*, 73–76.
- Squirrell, J. M.; Wokosin, D. L.; White, J. G.; Bavister, B. D. *Nat. Biotechnol.* **1999**, *17*, 763–767.
- Perry, J. W.; Mansour, K.; Lee, I. Y. S.; Wu, X. L.; Bedworth, P. V.; Chen, C. T.; Ng, D.; Marder, S. R.; Miles, P.; Wada, T.; Tian, M.; Sasabe, H. *Science* **1996**, *273*, 1533–1536.
- Said, A. A.; Wamsley, C.; Hagan, D. J.; Vanstryland, E. W.; Reinhardt, B. A.; Roderer, P.; Dillard, A. G. *Chem. Phys. Lett.* **1994**, *228*, 646–650.
- Starkey, J. R.; Rebane, A. K.; Drobizhev, M. A.; Meng, F.; Gong, A.; Elliott, A.; McInerney, K.; Spangler, C. W. *Clin. Cancer Res.* **2008**, *14*, 6564–6573.
- Birge, R. R.; Pierce, B. M. *J. Chem. Phys.* **1979**, *70*, 165–178.
- Bonin, K. D.; McIlrath, T. J. *J. Opt. Soc. Am. B* **1984**, *1*, 52–55.
- McClain, W. M. *J. Chem. Phys.* **1971**, *55*, 2789–2796.
- Wanapun, D.; Wampler, R. D.; Begue, N. J.; Simpson, G. J. *Chem. Phys. Lett.* **2008**, *455*, 6–12.
- Toro, C.; De Boni, L.; Lin, N.; Santoro, F.; Rizzo, A.; Hernandez, F. E. *Chirality* **2010**, *22*, E202–E210.
- Toro, C.; De Boni, L.; Lin, N.; Santoro, F.; Rizzo, A.; Hernandez, F. E. *Chem.–Eur. J.* **2010**, *16*, 3504–3509.
- Power, E. A. *J. Chem. Phys.* **1975**, *63*, 1348–1350.
- Tinoco, I. *J. Chem. Phys.* **1975**, *62*, 1006–1009.
- Vivas, M. G.; De Boni, L.; Bretonniere, Y.; Andraud, C.; Mendonca, C. R. *Opt. Express* **2012**, *20*, 18600–18608.
- Meath, W. J.; Power, E. A. *J. Phys. B: At., Mol. Opt. Phys.* **1984**, *17*, 763–781.
- Nascimento, M. A. C. *Chem. Phys.* **1983**, *74*, 51–66.
- Lazar, J.; Bondar, A.; Timr, S.; Firestein, S. J. *Nat. Methods* **2011**, *8*, 684–U120.
- Correa, D. S.; De Boni, L.; Misoguti, L.; Cohanoschi, I.; Hernandez, F. E.; Mendonca, C. R. *Opt. Commun.* **2007**, *277*, 440–445.
- Frisch, M. J.; Trucks, G. W.; Schlegel, H. B.; Scuseria, G. E.; Robb, M. A.; Cheeseman, J. R.; Scalmani, G.; Barone, V.; Mennucci, B.; Petersson, G. A.; et al. *Gaussian 09*, revision A.1.; Gaussian, Inc.: Wallingford, CT, 2009.
- Becke, A. D. *Phys. Rev. A* **1988**, *38*, 3098–3100.
- Becke, A. D. *J. Chem. Phys.* **1993**, *98*, 5648–5652.
- Lee, C. T.; Yang, W. T.; Parr, R. G. *Phys. Rev. B* **1988**, *37*, 785–789.
- Krishnan, R.; Binkley, J. S.; Seeger, R.; Pople, J. A. *J. Chem. Phys.* **1980**, *72*, 650–654.
- DALTON, a molecular electronic structure program, release 2.0 (2005); see <http://www.kjemi.uio.no/software/dalton/dalton.html>.
- Dunning, T. H. *J. Chem. Phys.* **1989**, *90*, 1007–1023.
- Tomasi, J.; Mennucci, B.; Cammi, R. *Chem. Rev.* **2005**, *105*, 2999–3093.
- Vivas, M. G.; Silva, D. L.; De Boni, L.; Zalesny, R.; Bartkowiak, W.; Mendonca, C. R. *J. Appl. Phys.* **2011**, *109*, 103529/1–103529/8.
- Silva, D. L.; Murugan, N. A.; Kongsted, J.; Rinkevicius, Z.; Canuto, S.; Ågren, H. *J. Phys. Chem. B* **2012**, *116*, 8169–8181.
- Rebane, A.; Drobizhev, M.; Makarov, N. S.; Beuerman, E.; Haley, J. E.; Douglas, M. K.; Burke, A. R.; Flikkema, J. L.; Cooper, T. M. *J. Phys. Chem. A* **2011**, *115*, 4255–4262.
- Vivas, M. G.; Silva, D. L.; De Boni, L.; Bretonniere, Y.; Andraud, C.; Laibe-Darbour, F.; Mulatier, J.-C.; Zalesny, R.; Bartkowiak, W.; Canuto, S.; Mendonca, C. R. *J. Phys. Chem. B* **2012**, *116*, 14677–14688.
- Vivas, M. G.; Mendonca, C. R. *J. Phys. Chem. A* **2012**, *116*, 7033–7038.
- Engel, E.; Koschorreck, M.; Leo, K.; Hoffmann, M. *Phys. Rev. Lett.* **2005**, *95*, 157403/1–157403/4.
- Rodriguez-Llorente, S.; Aroca, R.; Duff, J. *Spectrochim. Acta, Part A: Mol. Biomol. Spectrosc.* **1999**, *55*, 969–978.
- Piovesan, E.; Silva, D. L.; De Boni, L.; Guimaraes, F. E. G.; Misoguti, L.; Zalesny, R.; Bartkowiak, W.; Mendonca, C. R. *Chem. Phys. Lett.* **2009**, *479*, 52–55.
- Day, P. N.; Nguyen, K. A.; Pachter, R. *J. Phys. Chem. B* **2005**, *109*, 1803–1814.
- Ryderfors, L.; Mukhtar, E.; Johansson, L. B. A. *J. Phys. Chem. A* **2008**, *112*, 5794–5803.
- Knapp, E. W.; Fischer, S. F. *J. Chem. Phys.* **1981**, *74*, 89–95.